Journal of Intelligent and Robotic Systems **38:** 237–253, 2003.

Stable Adaptive Fuzzy Control with TSK Fuzzy Friction Estimation for Linear Drive Systems

LIH-CHANG LIN and JU-CHANG LAI
Department of Mechanical Engineering, National Chung Hsing University, Taichung, Taiwan 402, R.O.C.; e-mail: lclin@mail.nchu.edu.tw

(Received: 22 August 2001; in final form: 4 April 2003)

Abstract. This paper considers the control of a linear drive system with friction and disturbance compensation. A stable adaptive controller integrated with fuzzy model-based friction estimation and switching-based disturbance compensation is proposed via Lyapunov stability theory. A TSK fuzzy model with local linear friction models is suggested for real-time estimation of its consequent local parameters. The parameters update law is derived based on linear parameterization. In order to compensate for the effects resulting from estimation error and disturbance, a robust switching law is incorporated in the overall stable adaptive control system. Extensive computer simulation results show that the proposed stable adaptive fuzzy control system has very good performances, and is potential for precision positioning and trajectory tracking control of linear drive systems.

Key words: adaptive fuzzy control, TSK fuzzy friction model, Lyapunov stability, linear drive system, disturbance compensation.

1. Introduction

Consideration of the effects of nonlinear friction often plays an important role in the design of a precision motion control system [1, 6, 15, 19, 20]. Friction is a rather complex natural phenomenon and it is not yet completely understood. Usually, the classical friction models are described by static mappings between velocity and friction force. And classical friction model-based control can lead to large tracking errors, serious limit cycles, and undesired stick-slip motion [1, 4, 6].

Many studies (e.g., [1, 6, 8]) have shown that a dynamic friction model is necessary to describe the friction phenomena more accurately. Dahl [8] proposed a dynamic model for describing the spring-like behavior during stiction. Armstrong-Hélouvry [1] suggested a seven parameter model integrating the stiction and sliding friction models. Rice and Ruina [16] suggested another dynamic model not defined at zero velocity, and Dupont [9] used it for control design. Canudas de Wit et al. [6] proposed a dynamic friction model, called the LuGre model, that can capture most of the friction behavior including the Stribeck effect, hysteresis, spring-like characteristics for stiction, and varying break-away force. Recently, Swevers et al. [24] presented a new dynamic friction model that incorporates a hysteresis function with nonlocal memory and arbitrary transition curves for modeling presliding friction.

There have found great interests about adaptive friction compensation in motion control systems, e.g. [5, 12, 13, 17, 22, 25, 27, 28]. Walrath [25] suggested an adaptive compensation for bearing friction based on the Dahl model. Canudas de Wit et al. [5] proposed a composite control system composed of a linear controller and an adaptive nonlinear friction compensation for DC-motor drives. Yang and Tomizuka [27] presented an adaptive pulse width control for precise positioning with negligible backlash and flexibility. Nikiforuk and Tamura [13] considered the Coulomb friction as a disturbance and proposed a model reference adaptive control system for accommodating load variation and disturbance. Yang and Chu [28] proposed an adaptive PID velocity control with feedforward friction compensation for DC-motor drives. Ro and Hubbel [17] presented two stable model reference adaptive control laws: one for the presliding microdynamics of the elastic surface deflection and the other for the sliding macrodynamics. Smith et al. [22] suggested two adaptive control strategies for precision machine tool axis. Lin and Lin [12] proposed a stable adaptive control law for drive systems with transmission flexibility and friction, and then a fuzzy-enhancing strategy is used to improve system's transient performance and robustness.

In this paper, we first propose a TSK fuzzy model-based friction estimation structure that can be used for real-time nonlinear friction identification. Then a stable adaptive control strategy with TSK fuzzy friction and robust disturbance compensation for linear drive systems, is derived via the Lyapunov stability theory. The suggested control design method is tested using extensive computer simulations.

2. TSK Fuzzy Approximator for Nonlinear Friction

2.1. PHYSICAL FRICTION MODEL

Friction is usually considered as a function of velocity with four dynamic regimes: zero velocity, boundary lubrication, partial fluid lubrication, and full fluid lubrication [1]. Recently, Canudas de Wit et al. [6] proposed the LuGre dynamic friction model that can capture most of the real friction behavior, such as the Stribeck effect, hysteresis, spring-like characteristics for stiction, and varying break-away force. Based on the equivalent elastic bristles model for the contact surfaces of two rigid bodies, as shown in Figure 1, the average deflection z of the bristles is modeled by

$$\frac{\mathrm{d}z}{\mathrm{d}t} = v - \frac{|v|}{g(v)}z, \tag{1}$$

where v is the relative velocity between the two bodies, and $g(v)$ is a suitable positive function. For typical bearing friction, $g(v)$ will decrease monotonically from $g(0)$ when v increases, this is the so-called Stribeck effect. Thus, a parameterization of $g(v)$ for describing the Stribeck effect is

$$\sigma_0 g(v) = F_c + (F_s - F_c)\,\mathrm{e}^{-(v/v_s)^2}, \tag{2}$$

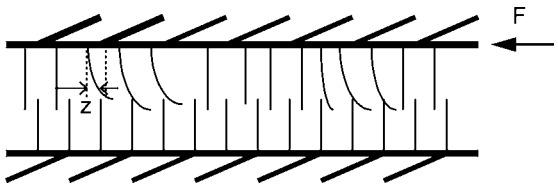

Figure 1. Bristles model for friction.

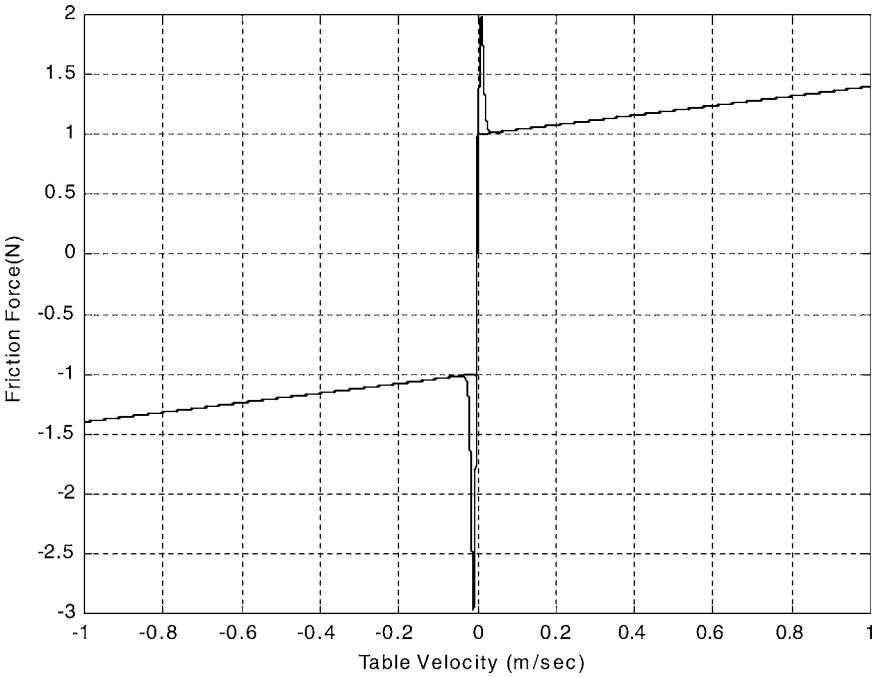

Figure 2. Friction versus velocity curve.

where F_c is the Coulomb friction, F_s is the stiction friction, and v_s is the Stribeck velocity [1, 6].

A dynamic friction model consisted of the friction force due to the contact bristles and the viscous force proportional to the relative velocity v can thus be described by

$$F_{\mathrm{f}} = \sigma_0 z + \sigma_1 \frac{\mathrm{d}z}{\mathrm{d}t} + \sigma_2 v, \tag{3}$$

where σ_0 and σ_1 are the equivalent stiffness and damping coefficient of the bristles, respectively; and σ_2 is the apparent viscous damping coefficient. The above friction model given by Equations (1)–(3) can accommodate different types of phenomena: presliding displacement, friction lag (hysteretic behavior), varying break-away force, and stick-slip motion [1, 6]. The relationship between the friction F_{f} and the relative velocity v is shown in Figure 2 using the following friction parameters [4]: $\sigma_0 = 10^5$ N/m, $\sigma_1 = \sqrt{10^5}$ N s/m, $\sigma_2 = 0.4$ N s/m, $F_c = 1$ N, $F_s = 1.5$ N,

$v_s = 0.001$ m/s. This friction model will be used for the computer simulations to illustrate the performance of the linear drive control system.

2.2. FRICTION APPROXIMATOR USING TSK FUZZY MODEL

Usually, there are two types of fuzzy rule-based models for function approximation: (1) the Mamdani model, and (2) the Takagi–Sugeno–Kang (TSK) model. The Mamdani model uses rules whose consequent part is a fuzzy set in the output's universe of discourse, however, the TSK model uses rules whose consequent part is a linear model. One of the main advantages of the TSK model is that it can approximate a complex nonlinear mapping using much fewer rules than the traditional Mamdani model [3, 23, 29].

Based on the friction versus velocity characteristics, we suggest a fuzzy friction estimator as shown in Figure 3, with a fuzzy rule-base consisting of the following TSK type of rules:

$$R_i: \quad \text{If } v(t) \text{ is } A_i \quad \text{Then } f_{\mathrm{f},i}(t) = c_i v(t) + d_i, \quad i = 1, 2, \ldots, M, \tag{4}$$

where $v(t)$ is the relative velocity, A_i is a fuzzy set defined in the normalized universe of discourse of v, $f_{\mathrm{f},i}(t)$ is the suggested friction by the ith rule, c_i and d_i are the parameters of the linear model in the consequent part, and M is the total number of fuzzy rules. The local linear models are used for piecewise approximation to the real nonlinear friction curve.

Fuzzy sets with parameterized membership function can be defined in the normalized universe of velocity v^* as shown in Figure 4, where nine triangular fuzzy

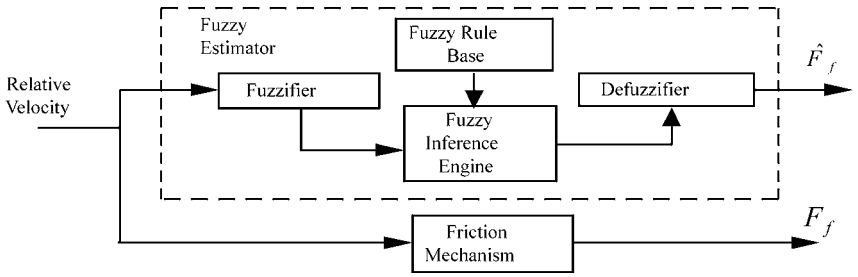

Figure 3. A fuzzy friction estimator.

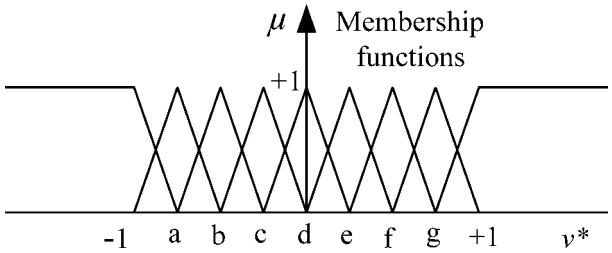

Figure 4. Fuzzy sets definition.

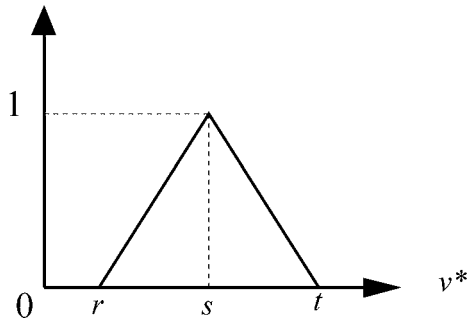

Figure 5. A triangular membership function.

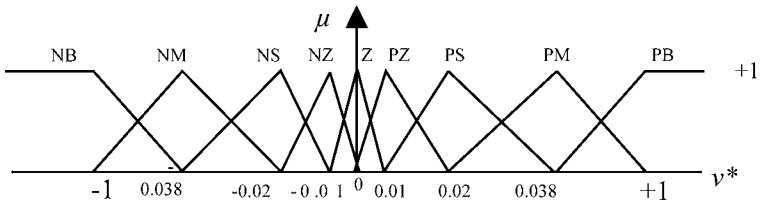

Figure 6. A typical definition for the fuzzy sets.

sets are defined. A triangular membership function in Figure 5 can be parameterized for easy computation as follows:

$$\mu(v^*; r, s, t) = \begin{cases} 0, & v^* < r, \\ \dfrac{(v^* - r)}{(s - r)}, & r \leqslant v^* \leqslant s, \\ \dfrac{(t - v^*)}{(t - s)}, & s \leqslant v^* \leqslant t, \\ 0, & v^* > t. \end{cases} \tag{5}$$

In this study, nine triangular fuzzy sets are defined as shown in Figure 6. In accordance with the real friction characteristics (refer to Figure 2) with Stribeck effect and thus highly nonlinear in the low speed region, more fuzzy sets are defined near the zero velocity. When $A_i = \text{PB}$, c_i is the viscous damping coefficient, and d_i is the Coulomb friction. As for $A_i = \text{PS}$, c_i can be negative to describe the Stribeck effect, and d_i means the intercept of the local tangent of the friction curve at this small velocity with the vertical axis.

The inference mechanism for the TSK fuzzy estimator is an interpolation of all the relevant linear models using the singleton fuzzifier and the center average defuzzifier [3, 23, 26, 29]. Thus, the estimate $\widehat{F}_{\text{f}}(t)$ for the friction can be computed as follows:

$$\widehat{F}_{\text{f}}(t) = \frac{\sum_{i=1}^{M} \mu_i f_{\text{f},i}(t)}{\sum_{i=1}^{M} \mu_i}, \tag{6}$$

where $\mu_i = \mu_{A_i}(v^*(t))$ is the matching degree of the antecedent part of ith rule with the current normalized velocity $v^*(t) = k_v v(t)$, k_v is the scaling factor for

the velocity, and $\mu_{A_i}(\cdot)$ is the membership function of the fuzzy set A_i. If the parameters for the antecedent parts of the TSK fuzzy friction estimator are fixed and only the consequent parameters c_i and d_i are to be learned, then Equation (6) can be represented as the well-known regression model:

$$\widehat{F}_{\mathrm{f}}(t) = \phi^{\mathrm{T}}(t)\theta(t), \tag{7}$$

where the regression vector is defined as

$$\begin{aligned}\phi^{\mathrm{T}}(t) &\equiv \left[\mu_1\psi^{\mathrm{T}}(t)\ \mu_2\psi^{\mathrm{T}}(t)\ \ldots\ \mu_M\psi^{\mathrm{T}}(t)\right],\\ \psi^{\mathrm{T}}(t) &\equiv \left[v^*(t)\ 1\right]\end{aligned} \tag{8}$$

and the unknown parameters vector is

$$\begin{aligned}\theta(t) &\equiv \left[\theta_1^{\mathrm{T}}(t)\ \theta_2^{\mathrm{T}}(t)\ \ldots\ \theta_M^{\mathrm{T}}(t)\right]^{\mathrm{T}},\\ \theta_i(t) &\equiv \left[c_i(t)\ d_i(t)\right]^{\mathrm{T}}, \quad i = 1, 2, \ldots, M.\end{aligned} \tag{9}$$

3. Stable Adaptive Fuzzy Control Design for Linear Drive Systems

In this study, we consider the linear drive systems shown in Figure 7(a), where the electromagnetic thrust force F_m generated from a permanent magnet linear synchronous motor (PMLSM) is directly applied to the platen (mover). The voltage equations of a PMLSM in terms of the equivalent synchronous rotating d–q frame (refer to Figure 7(b)) is as follows [10, 11, 14]:

$$v_q = R_s i_q + \dot{\lambda}_q + \omega_e \lambda_d, \tag{10}$$

$$v_d = R_s i_d + \dot{\lambda}_d - \omega_e \lambda_q \tag{11}$$

where

$$\lambda_q = L_q i_q, \tag{12}$$

$$\lambda_d = L_d i_d + \lambda_{\mathrm{PM}}, \tag{13}$$

$$\omega_e = n_p \omega_r \tag{14}$$

and v_d, v_q and i_d, i_q are respectively the d–q axis voltages and currents of the mover windings; R_s is the mover winding resistance; L_d and L_q are the d–q axis

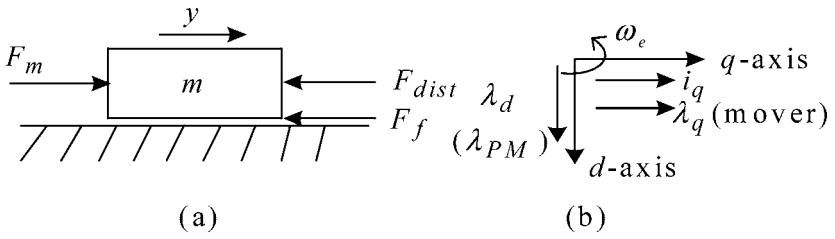

Figure 7. Schematic of a linear mover system.

inductances; ω_r is the mechanical angular velocity of the mover; ω_e is the electrical angular velocity; λ_{PM} is the permanent magnet flux linkage; n_p is the number of primary pole pairs. And

$$\omega_r = \frac{\pi v}{\tau}, \tag{15}$$

$$v_e = n_p v = 2\tau f_e \tag{16}$$

where v is the mechanical linear velocity of the mover, m/s; τ is the pole pitch, m; v_e is the electric linear velocity, m/s; f_e ($= \omega_e/2\pi$) is the electric frequency, Hz. The developed electromagnetic power is

$$P_m = F_m v = 3n_p\left[\lambda_d i_q + (L_d - L_q) i_d i_q\right]\frac{\omega_r}{2} \tag{17}$$

and the electromagnetic thrust force is thus

$$F_m = \frac{3\pi}{2\tau} n_p\left[\lambda_d i_q + (L_d - L_q) i_d i_q\right]. \tag{18}$$

Based on the field orientation principle [14] and using $i_d = 0$, then $\lambda_d = \lambda_{\mathrm{PM}} =$ constant, and the thrust force is proportional to the mover's q-axis current:

$$F_m = \frac{3\pi}{2\tau} n_p \lambda_{\mathrm{PM}} i_q = K_{\mathrm{f}} i_q \tag{19}$$

where K_{f} is the thrust coefficient of the linear motor.

Referring to Figure 7 and using the Newton's second law, the equation of motion for the mover of a linear drive system can be obtained as follows:

$$m\ddot{y}(t) + F_{\mathrm{f}}(t) + F_{\mathrm{dist}}(t) = F_m(t), \tag{20}$$

where $y(t)$ is the displacement of the mover; $F_{\mathrm{dist}}(t)$ is the external disturbance force, and $F_{\mathrm{f}}(t)$ is the friction force revisited as follows:

$$\begin{aligned} F_{\mathrm{f}} &= \sigma_0 z(t) + \sigma_1 \dot{z}(t) + \sigma_2 \dot{y}(t), \\ \dot{z}(t) &= \dot{y}(t) - \frac{|\dot{y}(t)|}{g(\dot{y})} z(t), \\ \sigma_0 g(\dot{y}(t)) &= F_c + (F_s - F_c)\, \mathrm{e}^{-(\dot{y}/v_s)^2}. \end{aligned} \tag{21}$$

Based on Equation (20), the structure of a computed force controller for arbitrary trajectory tracking can be selected as [7]

$$\begin{aligned} F_m(t) &= m f'_m(t) + \widehat{F}_{\mathrm{f}}(t) + F_{\mathrm{comp}}(t), \\ f'_m(t) &= \ddot{y}_d(t) + k_d \dot{e}(t) + k_p e(t) \end{aligned} \tag{22}$$

where $\widehat{F}_{\mathrm{f}}(t) = \phi^{\mathrm{T}}(t)\theta(t)$ is the real-time estimate for the friction to be designed later; $e(t) = y_d(t) - y(t)$, $y_d(t)$ is the desired trajectory; k_p and k_d are the proportional and derivative control gains, respectively; and $F_{\mathrm{comp}}(t)$ is to compensate

for the disturbance. Substituting (22) into (20), the error dynamics equation of the closed-loop system can be obtained as

$$\ddot{e}(t) + k_d\dot{e}(t) + k_p e(t) = \frac{1}{m}\big[F_{\mathrm{f}}(t) - \widehat{F}_{\mathrm{f}}(t)\big] + \frac{1}{m}\big[F_{\mathrm{dist}}(t) - F_{\mathrm{comp}}(t)\big]. \quad (23)$$

Define the tracking error vector and the parameters estimation error vector for the friction, respectively, as: $\boldsymbol{E}(t) = [e(t)\dot{e}(t)]^{\mathrm{T}}$ and $\boldsymbol{\theta}_e(t) = \boldsymbol{\theta}^* - \boldsymbol{\theta}(t)$, where $\boldsymbol{\theta}^*$ is the optimal parameters vector for the TSK fuzzy friction estimator, then, by (23), we have

$$\dot{\mathbf{E}}(t) = \begin{bmatrix} \dot{e}(t) \\ \ddot{e}(t) \end{bmatrix} = \boldsymbol{A}_e\boldsymbol{E} + \boldsymbol{B}_{\mathrm{f}} + \boldsymbol{B}_d - \boldsymbol{B}_c\boldsymbol{F}_{\mathrm{comp}} \quad (24)$$

where

$$\boldsymbol{A}_e = \begin{bmatrix} 0 & 1 \\ -k_p & -k_d \end{bmatrix}, \qquad \boldsymbol{B}_{\mathrm{f}} = \begin{bmatrix} 0 \\ \dfrac{F_{\mathrm{f}} - \widehat{F}_{\mathrm{f}}}{m} \end{bmatrix},$$

$$\boldsymbol{B}_d = \begin{bmatrix} 0 \\ \dfrac{F_{\mathrm{dist}}}{m} \end{bmatrix}, \quad \text{and} \quad \boldsymbol{B}_c = \begin{bmatrix} 0 \\ \dfrac{1}{m} \end{bmatrix}.$$

In the following, we will select a Lyapunov function candidate $V(\boldsymbol{E}, \theta_e)$ for the derivation of a stable adaptive control for the linear drive system via the Lyapunov stability theory [2, 23]:

$$V(\boldsymbol{E}, \theta_e) = \frac{1}{2}\boldsymbol{E}^{\mathrm{T}}\boldsymbol{P}\boldsymbol{E} + \frac{1}{2\gamma}\boldsymbol{\theta}_e^{\mathrm{T}}\boldsymbol{\theta}_e \quad (25)$$

where $\gamma > 0$, and

$$\boldsymbol{P} = \begin{bmatrix} \boldsymbol{p_1} \\ \boldsymbol{p_2} \end{bmatrix} = \begin{bmatrix} p_{11} & p_{12} \\ p_{21} & p_{22} \end{bmatrix}$$

is the symmetrical positive definite matrix satisfying the following Lyapunov equation:

$$\boldsymbol{A}_e^{\mathrm{T}}\boldsymbol{P} + \boldsymbol{P}\boldsymbol{A}_e = -\boldsymbol{Q} \quad (26)$$

where $\boldsymbol{Q}$ is a selected symmetric positive definite matrix, e.g., $\boldsymbol{Q} = \mathrm{diag}[q_{11}, q_{22}]$, $q_{11}, q_{22} > 0$. Taking the time derivative of $V(\boldsymbol{E}, \theta_e)$, we can obtain:

$$\begin{aligned} \dot{V}(\boldsymbol{E}, \theta_e) &= \frac{1}{2}(\dot{\boldsymbol{E}}^{\mathrm{T}}\boldsymbol{P}\boldsymbol{E} + \boldsymbol{E}^{\mathrm{T}}\boldsymbol{P}\dot{\boldsymbol{E}}) + \frac{1}{\gamma}\boldsymbol{\theta}_e^{\mathrm{T}}\dot{\boldsymbol{\theta}}_e \\ &= -\frac{1}{2}\boldsymbol{E}^{\mathrm{T}}\boldsymbol{Q}\boldsymbol{E} + \boldsymbol{B}_{\mathrm{f}}^{\mathrm{T}}\boldsymbol{P}\boldsymbol{E} + \boldsymbol{B}_d^{\mathrm{T}}\boldsymbol{P}\boldsymbol{E} + \frac{1}{\gamma}\boldsymbol{\theta}_e^{\mathrm{T}}\dot{\boldsymbol{\theta}}_e - \boldsymbol{B}_c^{\mathrm{T}}\boldsymbol{P}\boldsymbol{E}\boldsymbol{F}_{\mathrm{comp}} \\ &= -\frac{1}{2}\boldsymbol{E}^{\mathrm{T}}\boldsymbol{Q}\boldsymbol{E} + \frac{1}{m}(F_{\mathrm{f}} - \widehat{F}_{\mathrm{f}})\boldsymbol{p_2}\boldsymbol{E} + \frac{1}{m}F_{\mathrm{dist}}\boldsymbol{p_2}\boldsymbol{E} \\ &\quad + \frac{1}{\gamma}\boldsymbol{\theta}_e^{\mathrm{T}}\dot{\boldsymbol{\theta}}_e - \frac{1}{m}F_{\mathrm{comp}}\boldsymbol{p}_2\boldsymbol{E}. \end{aligned} \quad (27)$$

Since $\widehat{F}_{\mathrm{f}}(t)$ can be parameterized as

$$\widehat{F}_{\mathrm{f}}(t) = \widehat{F}_{\mathrm{f,opt}}(t) - \left[\widehat{F}_{\mathrm{f,opt}}(t) - \widehat{F}_{\mathrm{f}}(t)\right] = \phi^{\mathrm{T}}(t)\boldsymbol{\theta}^* - \phi^{\mathrm{T}}(t)\boldsymbol{\theta}_e(t). \tag{28}$$

Equation (27) can then be expressed as

$$\begin{aligned}\dot{V}(\boldsymbol{E}, \theta_e) = &-\frac{1}{2}\boldsymbol{E}^{\mathrm{T}}\boldsymbol{Q}\boldsymbol{E} + \frac{1}{m}\phi^{\mathrm{T}}(t)\boldsymbol{\theta}_e(t)\boldsymbol{p}_2\boldsymbol{E} + \frac{1}{\gamma}\boldsymbol{\theta}_e^{\mathrm{T}}\dot{\boldsymbol{\theta}}_e + \frac{1}{m}F_{\mathrm{dist}}\boldsymbol{p}_2\boldsymbol{E} \\ &+ \frac{1}{m}(F_{\mathrm{f}} - \widehat{F}_{\mathrm{f,opt}}(t))\boldsymbol{p}_2\boldsymbol{E} - \frac{1}{m}F_{\mathrm{comp}}\boldsymbol{p}_2\boldsymbol{E}.\end{aligned} \tag{29}$$

Based on Equation (29), we can choose the parameters adaptation law for the TSK fuzzy friction estimator $\dot{\boldsymbol{\theta}}(t)$ as

$$\dot{\boldsymbol{\theta}}(t)(= -\dot{\boldsymbol{\theta}}_e(t)) = \frac{\gamma}{m}\phi(t)\boldsymbol{p}_2\boldsymbol{E}, \quad \gamma > 0, \tag{30}$$

and the disturbance and uncertainty compensation F_{comp} as

$$F_{\mathrm{comp}} = m(D^u + \varepsilon)\mathrm{sgn}(\boldsymbol{p}_2\boldsymbol{E}) \tag{31}$$

where mD^u and $m\varepsilon$ are respectively the upper bounds of the disturbance and the minimal friction estimation error,

$$\frac{1}{m}|F_{\mathrm{dist}}| \leqslant D^u, \tag{32}$$

$$\frac{1}{m}|F_{\mathrm{f}} - \widehat{F}_{\mathrm{f,opt}}(t)| \leqslant \varepsilon. \tag{33}$$

And the resulting time derivative of V is

$$\begin{aligned}\dot{V}(\boldsymbol{E}, \theta_e) = &-\frac{1}{2}\boldsymbol{E}^{\mathrm{T}}\boldsymbol{Q}\boldsymbol{E} + \frac{1}{m}\left|F_{\mathrm{f}} - \widehat{F}_{\mathrm{f,opt}}(t)\right|\boldsymbol{p}_2\boldsymbol{E} + \frac{F_{\mathrm{dist}}}{m}\boldsymbol{p}_2\boldsymbol{E} \\ &- \boldsymbol{p}_2\boldsymbol{E}(D^u + \varepsilon)\mathrm{sgn}(\boldsymbol{p}_2\boldsymbol{E}) \leqslant 0\end{aligned} \tag{34}$$

where

$$\begin{aligned}&\frac{1}{m}\left|F_{\mathrm{f}} - \widehat{F}_{\mathrm{f,opt}}(t)\right|\boldsymbol{p}_2\boldsymbol{E} + \frac{F_{\mathrm{dist}}}{m}\boldsymbol{p}_2\boldsymbol{E} - \boldsymbol{p}_2\boldsymbol{E}(D^u + \varepsilon)\mathrm{sgn}(\boldsymbol{p}_2\boldsymbol{E}) \\ &\quad = \begin{cases} \left[\dfrac{1}{m}(F_{\mathrm{f}} - \widehat{F}_{\mathrm{f,opt}}) + \dfrac{F_{\mathrm{dist}}}{m}\right]\boldsymbol{p}_2\boldsymbol{E} - (D^u + \varepsilon)\boldsymbol{p}_2\boldsymbol{E} < 0, & \text{if } \boldsymbol{p}_2\boldsymbol{E} > 0, \\ 0, & \text{if } \boldsymbol{p}_2\boldsymbol{E} = 0, \\ \left[\dfrac{1}{m}(F_{\mathrm{f}} - \widehat{F}_{\mathrm{f,opt}}) + \dfrac{F_{\mathrm{dist}}}{m}\right]\boldsymbol{p}_2\boldsymbol{E} + (D^u + \varepsilon)\boldsymbol{p}_2\boldsymbol{E} < 0, & \text{if } \boldsymbol{p}_2\boldsymbol{E} < 0. \end{cases}\end{aligned} \tag{35}$$

By the LaSalle's theorem [2, 18, 21, 23], $\boldsymbol{E}(t) \to 0$ as $t \to 0$. Thus the arbitrary trajectory tracking control objective can be fulfilled by the derived adaptive fuzzy control consisting of Equations (22), (7), (8), (30) and (31). Since $V(\boldsymbol{E}, \theta_e)$

is positive and lower bounded, $\boldsymbol{\theta}_e(t)$ would be bounded, i.e., the estimation error would be only bounded and not necessarily approach to zero. In other words the tracking control performance can be rather satisfactory, however, the friction estimation error still exists. This is the usual situation of a stable adaptive control since the reference input is not with sufficient persistent excitation (PE). The friction estimation error can be further compensated for with the robust compensation law. It can be seen in the following simulation study.

Since the switching law in (31) will cause undesirable chattering in the control signal and involve high control activity, a thin boundary layer neighboring the switching surface $\boldsymbol{p_2 E} = 0$ can be introduced to eliminate the chattering. That is, the switching function $\text{sgn}(\boldsymbol{p_2 E})$ can be replaced by a saturation function:

$$\text{sat}(\boldsymbol{p_2 E}/\phi_b) = \begin{cases} -1 & \text{if } \boldsymbol{p_2 E}/\phi_b \leqslant -1, \\ \boldsymbol{p_2 E}/\phi_b & \text{if } -1 < \boldsymbol{p_2 E}/\phi_b \leqslant 1, \\ 1 & \text{if } \boldsymbol{p_2 E}/\phi_b > 1 \end{cases} \tag{36}$$

where ϕ_b is the thickness of the boundary layer, and the compensating control law becomes

$$F_{\text{comp}}(t) = m(D^u + \varepsilon)\text{sat}(\boldsymbol{p_2 E}/\phi_b). \tag{37}$$

4. Simulation Examples

In this section performance of the proposed adaptive control with TSK fuzzy friction estimation for linear drive systems will be tested using computer simulation. The LuGre dynamic friction model [6] is used in the plant dynamics model for illustrating the effectiveness of the suggested control strategy. In the simulations, the friction parameters and the definition of the fuzzy sets listed before, and following other parameters for the plant and controller are used: $m = 5$ kg, $\gamma = 2{,}250{,}000$, $D^u = 0.2$, $\varepsilon = 0.01$, $q_{11} = 4{,}000$, $q_{22} = 2{,}000$, $k_p = 2{,}500$, $k_d = 100$, $p_{21} = q_{11}/(2k_p)$, $p_{22} = (q_{22} + q_{11}/k_p)/(2k_d)$, $\phi_b = 0.001$. And the desired trajectory $y_d(t)$ is selected as shown in Figure 8(a).

Simulation results for the case of no disturbance tracking are shown in Figure 8. From Figures 8(a)–(c), we know that the suggested adaptive control law has very good tracking performance. The tracking error is approximately within ± 0.0011 mm. From Figures 8(d) and (e), we also know that the friction estimate using the real-time TSK fuzzy friction estimator can follow the real friction in this nominal control case. The control force shown in Figure 8(f) contains no chattering.

The following two disturbance forces, shown in Figures 9(a) and (b):

$$\begin{aligned} F_{\text{dist}}(t) = \frac{1}{10}(&2\sin(10t) - \cos(5t) - \sin(5t) + \cos(2.5t) + 2\sin(t) \\ &+ 2\cos(2t) + 2\sin(20t) - \cos(3.5t) - \sin(1.5t) + \cos(0.5t) \\ &+ 2\sin(0.01t) + 2\cos(22t)), \end{aligned} \tag{38a}$$

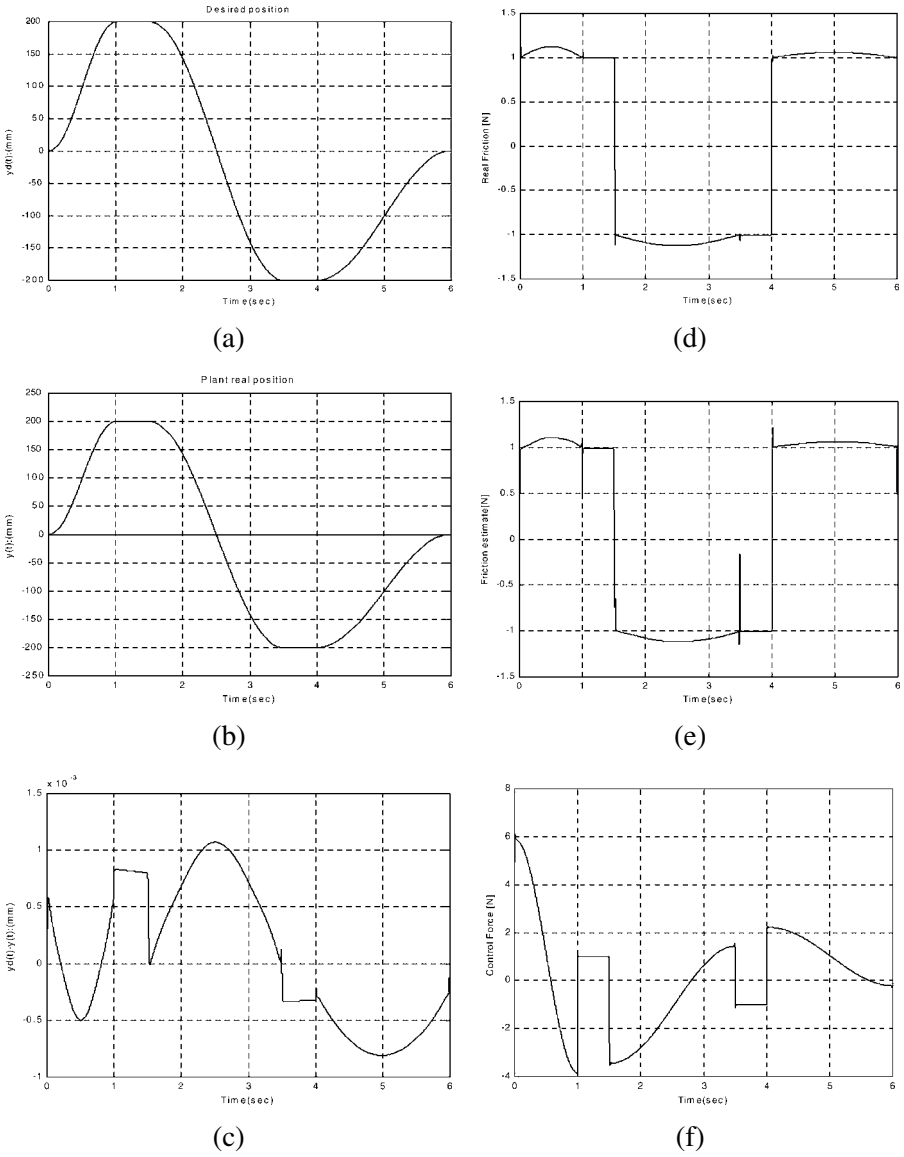

Figure 8. Simulation results for the case with no disturbance: (a) desired trajectory; (b) actual trajectory; (c) tracking error; (d) real friction; (e) friction estimate; (f) control force.

$$F_{\text{dist}}(t) = 2\sin(10t) - \cos(5t) - \sin(5t) + \cos(2.5t) + 2\sin(t) + 2\cos(2t) + 2\sin(20t) - \cos(3.5t) - \sin(1.5t) + \cos(0.5t) + 2\sin(0.01t) + 2\cos(22t) \tag{38b}$$

are considered in the following two simulation studies. Simulation results for the case with smaller disturbance force (38a) are shown in Figure 10. Figures 10(a)–(c)

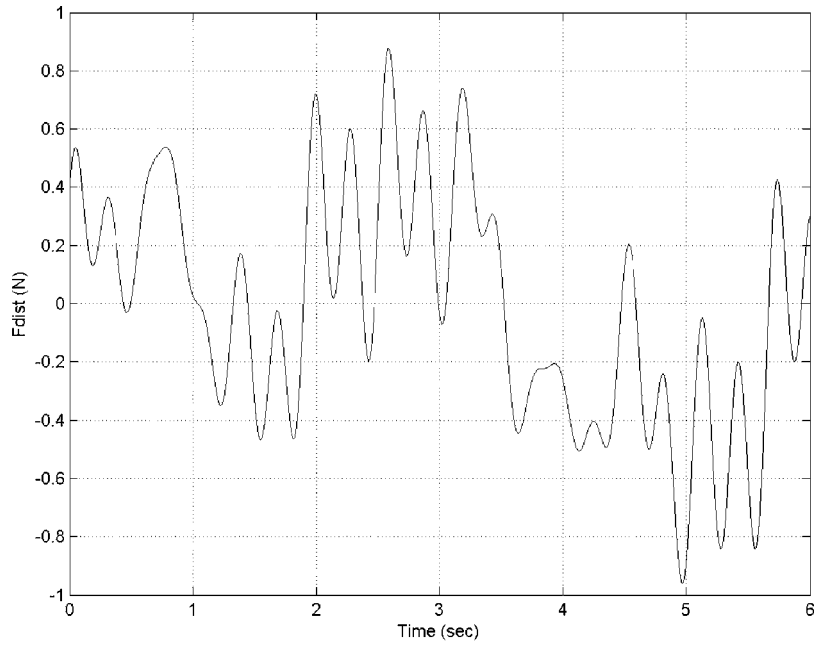

(a)

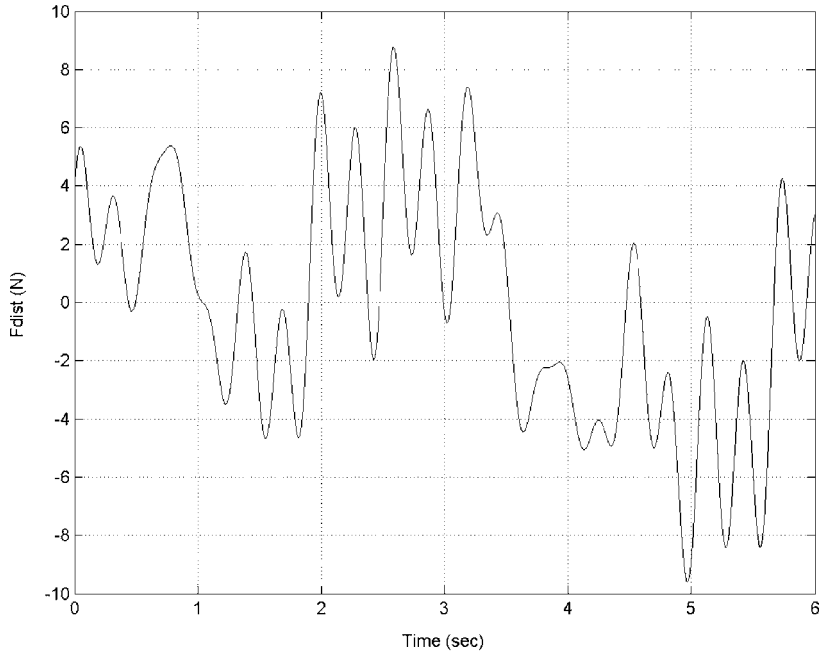

(b)

Figure 9. Two disturbance forces used in the simulations.

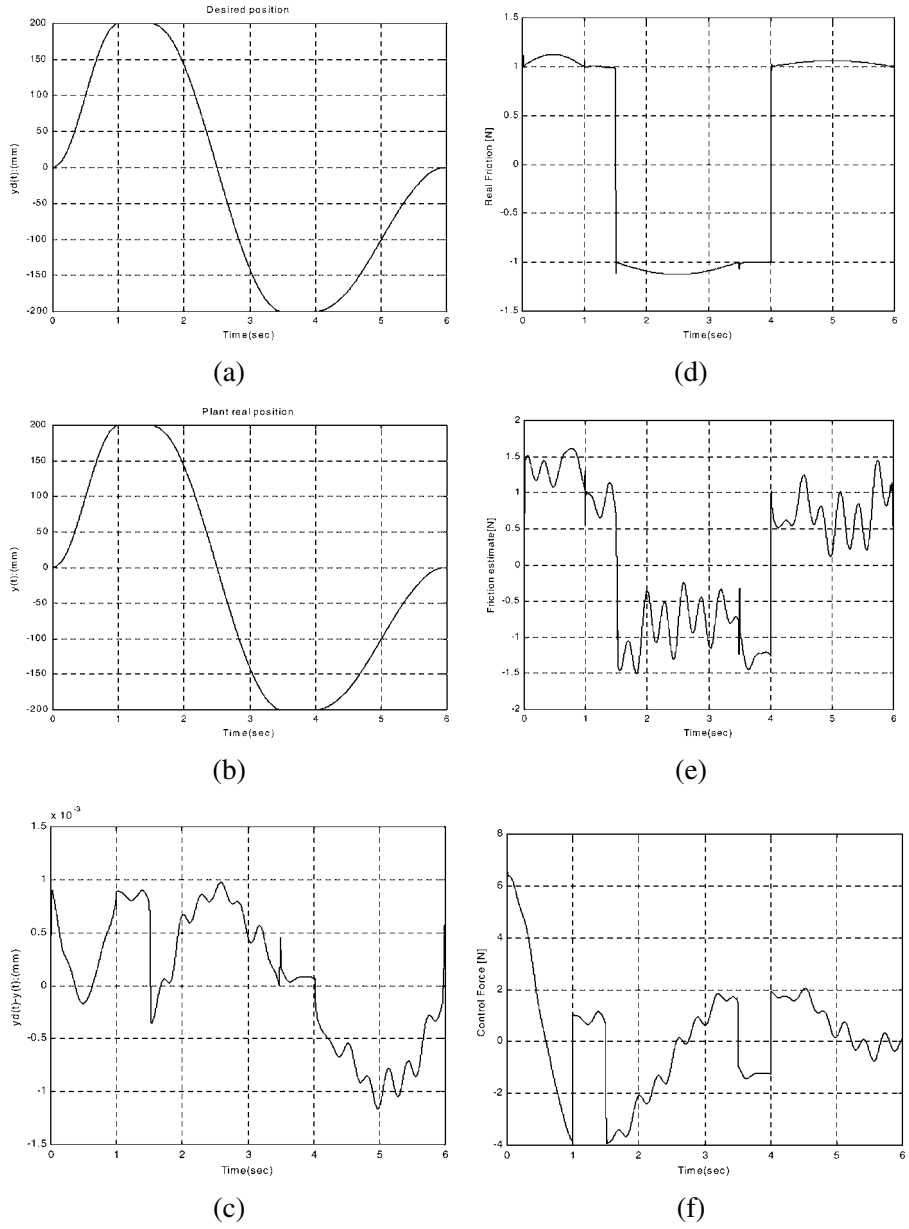

Figure 10. Simulation results for the case with smaller disturbance: (a) desired trajectory; (b) actual trajectory; (c) tracking error; (d) real friction; (e) friction estimate; (f) control force.

show that the suggested adaptive fuzzy control strategy has very good tracking performance. The tracking error is approximately within ± 0.0012 mm. Figures 10(d) and (e) show that the friction estimate using the real-time TSK fuzzy friction estimator can only approximately follow the real friction, however, the control objective can be attained. The control force with no chattering is shown in Figure 10(f).

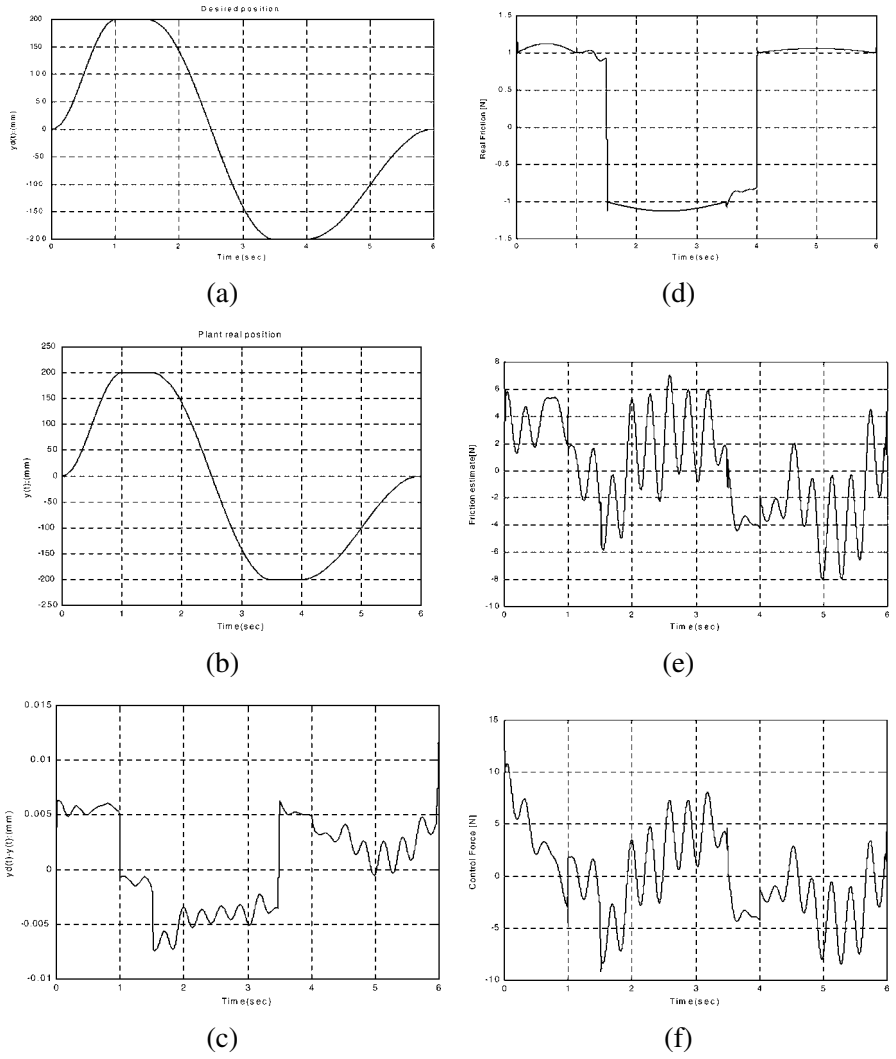

Figure 11. Simulation results for the case with larger disturbance: (a) desired trajectory; (b) actual trajectory; (c) tracking error; (d) real friction; (e) friction estimate; (f) control force.

Simulation results for the case with larger disturbance force (38b) are shown in Figure 11. Figures 11(a)–(c) show that the suggested adaptive fuzzy control strategy still has very good tracking performance. The tracking error is approximately within ± 0.0075 mm, however, the error becomes larger as time approaches 6 seconds due to near zero speed motion. Figures 11(d) and (e) show that the friction estimate using the real-time TSK fuzzy friction estimator cannot follow the real friction, however, the control system still has good performance. The control force with no ringing is shown in Figure 11(f).

To understand the constant speed control characteristics, Figure 12 shows the simulation results using the reference command $y_d(t) = 0.05t$, $0 \leqslant t \leqslant 2$. The

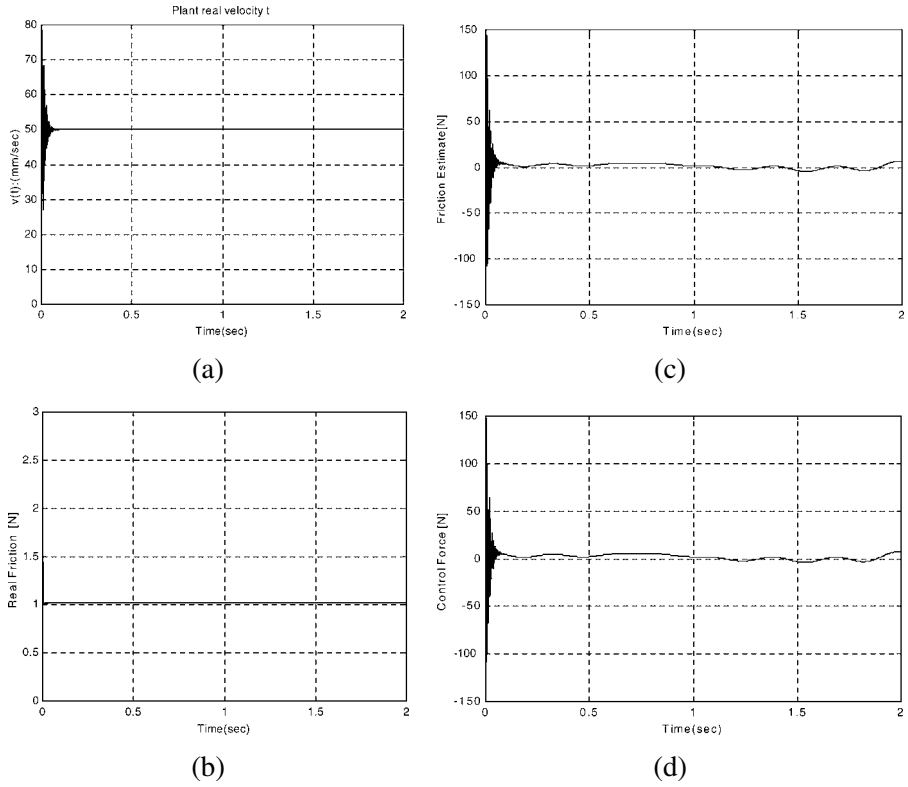

Figure 12. Simulation results for the constant speed control case with larger disturbance: (a) actual velocity; (b) real friction; (c) friction estimate; (d) control force.

thickness of the boundary layer is set to be $\phi_b = 0.1$, and the larger disturbance force (38b) is used in this simulation study. The real friction and real-time fuzzy friction estimate are shown in Figures 12(b) and (c), respectively. Due to the used larger disturbance force, the friction estimate could not converge to the real friction. However, from Figure 12(a), we know that the constant speed control objective could be well fulfilled. The control force with no ringing is shown in Figure 12(d).

5. Conclusions

Control strategies for precision motion systems need a suitable friction model to predict and compensate for the friction. This paper considers the adaptive control of a linear drive system with friction and disturbance compensation. A TSK fuzzy friction model with local linear models is first suggested and expressed in linear parameterization form for easy derivation of its parameters update law. Then a stable adaptive controller with fuzzy friction and robust disturbance compensation is proposed, based on the Lyapunov stability theory. In order to compensate for the effects resulting from real-time estimation error and disturbance, a

saturation function-based robust switching law is incorporated in the overall stable adaptive control system. Extensive computer simulations are used to validate the effectiveness of the proposed control strategy. For simplicity, the proposed TSK fuzzy friction model identification structure considers only one input variable, i.e., the platen velocity, thus the complex presliding microdynamics and its hysteretic behavior [24] deserve further study for constructing a more accurate presliding friction estimator. And it will have great potential for micropositioning applications.

Acknowledgements

This research was supported by National Science Council of R.O.C. under Grant NSC 89-2212-E-005-027. The authors would like to thank the referees for their constructive comments.

References

1. Armstrong-Hélouvry, B.: *Control of Machines with Friction*, Kluwer Academic Publishers, Boston, 1991.
2. Åström, K. J. and Wittenmark, B.: *Adaptive Control*, Addison-Wesley, New York, 2nd edn, 1995.
3. Babuška, R.: *Fuzzy Modeling for Control*, Kluwer Academic Publishers, Boston, 1998.
4. Bowden, F. P. and Leben, L.: The nature of sliding and the analysis of friction, *Proc. Roy. Soc. Ser. A* **169** (1953), 371–373.
5. Canudas de Wit, C., Åström, K. J., and Braun, K.: Adaptive friction compensation in DC-motor drives, *IEEE Trans. Robotics Automat.* **3**(6) (1987), 681–685.
6. Canudas de Wit, C., Olsson, H., Åström, K. J., and Lischinsky, P.: A new model for control of systems with friction, *IEEE Trans. Automat. Control* **40**(3) (1995), 419–425.
7. Craig, J. J.: *Introduction to Robotics: Mechanics and Control*, 2nd edn, Addison-Wesley, New York, 1989.
8. Dahl, P.: A solid friction model, Technical Report TOR-0158(3107-18)-1, Aerospace Corporation, El Segundo, CA, 1968.
9. Dupont, P. E.: Avoiding stick-slip through PD control, *IEEE Trans. Automat. Control* **39**(5) (1994), 1094–1097.
10. Guo, Q., Guo, W., Zhou, Y., and Wang, L.: Preview feedforward compensation of permanent magnet linear synchronous motor servo system implemented with Adaline, in: *IEEE 6th Internat. Workshop on Advanced Motion Control*, 2000, pp. 576–579.
11. Lin, C. H., Chou, W. D., and Lin, F. J.: Adaptive hybrid control using a recurrent neural network for a linear synchronous motor servo-drive system, *IEE Proc. Control Theory Appl.* **148**(2) (2001), 156–168.
12. Lin, L. C. and Lin, Y. J.: Fuzzy-enhanced adaptive control for flexible drive system with friction using genetic algorithms, *J. Intelligent Robotic Systems* **23** (1998), 379–405.
13. Nikiforuk, P. N. and Tamura, K.: Design of a disturbance accommodating adaptive control system and its application to a DC-servo motor system with Coulomb friction, *ASME J. Dyn. Systems Measm. Control* **110** (1988), 343–349.
14. Novotny, D. W. and Lipo, T. A.: *Vector Control and Dynamics of AC Drives*, Oxford, New York, 1997.

15. Ohnishi, K., Shibata, M., and Muraami, T.: Motion control for advanced mechatronics, *IEEE/ASME Trans. Mechatronics* **1**(1) (1996).
16. Rice, J. R. and Ruina, A. L.: Stability of steady frictional slipping, *J. Appl. Mech.* **50**(2) (1983).
17. Ro, P. I. and Hubbel, P. I.: Model reference adaptive control of dual-mode micro/macro dynamics of ball screws for nanometer motion, *ASME J. Dyn. Systems Measm. Control* **115** (1993), 103–108.
18. Sastry, S.: *Nonlinear Systems: Analysis, Stability, and Control*, Springer, New York, 1999.
19. Senturia, S. D.: *Microsystem Design*, Kluwer Academic Publishers, Boston, 2001.
20. Slocum, A. H.: *Precision Machine Design*, Prentice-Hall, Englewood Cliffs, NJ, 1992.
21. Slotine, J. E. and Li, W.: *Applied Nonlinear Control,* Prentice-Hall, Englewood Cliffs, NJ, 1991.
22. Smith, M. H., Annaswamy, A. M., and Slocum, A. H.: Adaptive control strategies for precision machine tool axis, *Precision Engrg.* **17**(3) (1995), 192–206.
23. Spooner, J. T., Maggiore, M., Ordóñez, R., and Passino, K. M.: *Stable Adaptive Control and Estimation for Nonlinear Systems: Neural and Fuzzy Approximator Techniques*, Wiley-Interscience, New York, 2002.
24. Swevers, J., Al-Bender, F., Ganseman, C. G., and Prajogo, T.: An integrated friction model structure with improved presliding behavior for accurate friction compensation, *IEEE Trans. Automat. Control* **45**(4) (2000), 675–686.
25. Walrath, C. D.: Adaptive bearing friction compensation based on recent knowledge of dynamic friction, *Automatica* **20** (1984), 717–727.
26. Wang, L. X.: *A Course in Fuzzy Systems and Control*, Prentice-Hall, Englewood Cliffs, NJ, 1997.
27. Yang, S. and Tomizuka, M.: Adaptive pulse width control for precise positioning under the influence of stiction and Coulomb friction, *ASME J. Dyn. Systems Measm. Control* **110** (1988), 221–227.
28. Yang, Y. P. and Chu, J. S.: Adaptive velocity control of DC motors with Coulomb friction identification, *ASME J. Dyn. Systems Measm. Control* **115** (1993), 95–102.
29. Yen, J. and Langari, R.: *Fuzzy Logic*: *Intelligence, Control, and Information,* Prentice-Hall, Englewood Cliffs, NJ, 1999.